Inorganica Chimica Acta, 121 (1986) 147–153

Mass Spectrometry of Complexes with Metal–Carbon σ Bonds. Part I. The Electron Impact Behavior of Some Allyl Complexes and their Cycloaddition Products

R. BERTANI, A. M. MACCIONI, P. TRALDI

C.N.R. Centro di Chimica Metallorganica e Area della Ricerca, Padua, Italy

and G. CARTURAN

Facoltà di Ingegneria, Università di Trento, Mesiano, Trento, Italy

(Received April 15, 1986; revised July 2, 1986)

Abstract

Electron Impact (EI) mass spectrometric behavior of $[\mathrm{PtCl}(\eta^1\text{-}\mathrm{C_3H_5})(\mathrm{L_2})]$ ($\mathrm{L_2} = 2\mathrm{PPh_3}, \mathrm{Ph_2P{-}C_2H_2{-}PPh_2}$) and $\{\mathrm{PtCl}[\overline{\mathrm{CH{-}CH_2{-}C(CN)_2{-}C(CN)_2{-}CH_2}}](\mathrm{L_2})\}$ are described and discussed in detail with the aid of linked scans exact mass measurements and collisional experiments. The cases of $[\mathrm{Mn}(\eta^1\text{-}\mathrm{C_3H_5})(\mathrm{CO})_5]$ and $\{\mathrm{Mn}[\overline{\mathrm{CH{-}CH_2{-}C(CN)_2{-}C(CN)_2{-}CH_2}}](\mathrm{CO})_5\}$ are also reported. Results are interpreted in terms of the different stability of η^1-allyl complexes as a function of coordinated ligands and of the possibility of η^3-allyl bond formation; these data are compared with mass spectrometric features of the corresponding cyclopentyl derivatives. For the latter a retro-synthetic reaction to tetracyanoethylene and the original allyl complex is described.

Introduction

The presence of a free double bond leads to substantial differences in reactivity between η^1-allyl complexes and ordinary alkyl complexes. A typical example is the |2 + 3| cycloaddition reaction of tetracyanoethylene (TCNE) to the η^1-allyl group [1–3]. In this reaction, the reactivity of the η^1-allyl group and the mechanism of the entire process are dictated by the nature of the η^1-allyl complex, so that the metal coordination environment ultimately determines the reaction path [4]. These facts prompted us to make an investigation of the mass spectrometric behavior of various η^1-allyl complexes. The study was completed by an examination of the corresponding TCNE and $\mathrm{CH_2{=}CH{-}CH_2{-}}$ cycloaddition products which should behave as typical σ metal–C complexes. In other words, to provide a general understanding of the role of the coordination sphere in determining the chemical properties of η^1-allyl complexes, we wished to compare their mass spectrometric behavior with that of the relevant 'allyl + TCNE' products. This work reports the EI mass spectrometric behavior of $[\mathrm{PtCl}(\eta^1\text{-}\mathrm{C_3H_5})(\mathrm{L_2})]$ ($\mathrm{L_2} = 2\mathrm{PPh_3}, \mathrm{Ph_2P{-}C_2H_2{-}PPh_2}$), $[\mathrm{Mn}(\eta^1\text{-}\mathrm{C_3H_5})(\mathrm{CO})_5]$ and the relevant products of |2 + 3| cycloaddition with TCNE, which have not previously been studied with the aid of linked scans [5], exact mass measurements and collisional experiments [6].

Experimental

Materials, Instrumentation and General Procedures

The working technique for air- and moisture-sensitive compounds was used for complex synthesis and sample preparation [7]. Solvents were dried according to literature methods and kept under argon atmosphere [8].

The tetramer $[\mathrm{PtCl(C_3H_5)}]_4$ [9], $[\mathrm{PtCl}(\eta^3\text{-}\mathrm{C_3H_5})(\mathrm{PPh_3})]$ [10] and the complex $[\mathrm{Mn}(\eta^1\text{-}\mathrm{C_3H_5})(\mathrm{CO})_5]$ [11] (**1c**) were prepared by known procedures. *trans*-$[\mathrm{PtCl}(\eta^1\text{-}\mathrm{C_3H_5})(\mathrm{PPh_3})_2]$ (**1a**) and $[\mathrm{PtCl}(\eta^1\text{-}\mathrm{C_3H_5})(\mathrm{Ph_2P{-}C_2H_2{-}PPh_2})]$ (**1b**) were obtained as reported previously [4]. *trans*-$\{\mathrm{PtCl}[\overline{\mathrm{CHCH_2C(CN)_2C(CN)_2CH_2}}](\mathrm{PPh_3})_2\}$ (**2a**) and $\{\mathrm{PtCl}[\overline{\mathrm{CHCH_2C(CN)_2C(CN)_2CH_2}}](\mathrm{PhP{-}C_2H_2{-}PPh_2})\}$ (**2b**) were prepared according to literature procedures and identified by comparison of ^{1}H and ^{31}P NMR spectra with reported data [4].

Infrared spectra were recorded on a Perkin Elmer Model 983 spectrophotometer as Nujol mulls using CsI windows or in $\mathrm{CCl_4}$ solution; spectra were calibrated with reference to polystyrene absorption at 1601 cm^{-1}.

The ^{1}H NMR spectra were recorded on a Varian FT 80 A instrument in $\mathrm{CD_3C_6D_5}$ or $\mathrm{CD_2Cl_2}$ solution. The ^{31}P {^{1}H} spectra were recorded on the same instrument operating at 32.204 MHz.

0020-1693/86/$3.50

Preparation of $\{Mn[\overline{CHCH_2C(CN)_2C(CN)_2CH_2}](CO)_5\}$ *(2c)*

An Et_2O suspension of $[Mn(\eta^1\text{-}C_3H_5)(CO)_5]$ (0.35 g, 1.48 mmol, 10 ml of solvent) was treated at −78 °C with an equivalent amount of TCNE (0.19 g) under nitrogen. After two days a whitish-yellow solid separated from the yellow solution and it was filtered off, washed with Et_2O and dried at reduced pressure (0.39 g, 72% yield).

Anal. Found: C, 45.7; H, 1.4; N, 15.2%. Calc. for $MnC_{14}H_5N_4O_5$: C, 46.17; H, 1.40; N, 15.40%.

Mass Spectrometric Procedures

All mass spectrometric measurements were performed on a VG ZAB 2F instrument [12] operating in electron impact (EI) mode (70 eV, 200 A). Compounds **1a**, **1b**, **1c** and **2a**, **2b**, **2c** were introduced under direct electron impact mode (DEI) [13] conditions, with a source temperature of 200 °C. Collisionally activated decomposition mass-analyzed ion kinetic energy (CAD MIKE) [6] spectra were obtained by 8 keV ions colliding with air in the second field free region. Pressure in the collisional chamber was such as to reduce main beam intensity at 40% of its usual value. Metastable transitions were detected by B/E linked scan experiments [5] which are indicated in the schemes by asterisks. Exact mass measurements were performed by peak matching techniques at 20 000 resolving power (10% valley definition). Kinetic energy release values ($T_{1/2}$) were calculated from the usual formula [14].

Results and Discussion

Preparation and Characterization of Complexes

The complexes *trans*-$[PtCl(\eta^1\text{-}C_3H_5)(PPh_3)_2]$ (**1a**), $[PtCl(\eta^1\text{-}C_3H_5)(Ph_2P{-}C_2H_2{-}PPh_2)]$ (**1b**), and $[Mn(\eta^1\text{-}C_3H_5)(CO)_5]$ (**1c**), were prepared according to literature procedures and characterized by IR, ^1H and ^{31}P $\{^1H\}$ NMR spectroscopy. The |2 + 3| cycloaddition products of TCNE and the η^1-allyl group were obtained by reaction (1):

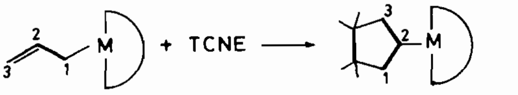

(1)

The complexes *trans*-$\{PtCl[\overline{CHCH_2C(CN)_2C(CN)_2CH_2}](PPh_3)_2\}$ (**2a**) and $\{PtCl[\overline{CHCH_2C(CN)_2C(CN)_2CH_2}](Ph_2P{-}C_2H_2{-}PPh_2)\}$ (**2b**) were previously known. The new complex $\{Mn[\overline{CHCH_2C(CN)_2C(CN)_2CH_2}](CO)_5\}$ (**2c**) was identified by elemental analysis and spectroscopic data. It is a whitish compound indefinitely stable at low temperature or under inert atmosphere, but slowly decomposes in air at room temperature. Its IR spectrum shows in CCl_4 solution a simple $\nu(C{\equiv}N)$ band at 2252 cm^{-1} and three absorptions in the range 2122–1992 cm^{-1} attributed to CO stretchings. The ^1H NMR spectrum provides informations revealing the |2 + 3| cycloaddition of TCNE to the allylic ligand with a 1–2 shift of the Mn–C σ bond. Figure 1 shows the spectrum in CD_2Cl_2: the five protons of the 'TCNE + allyl' group appear as three separate groups of signals, *x*, *y*, *z*, with intensity ratios of 2:2:1. The spectrum was interpreted on the basis of the AA′BB′C spin system; iterative computer modifications of relevant coupling constants led to a good simulated spectrum (Fig. 1b). Data are reported in Table I, which also

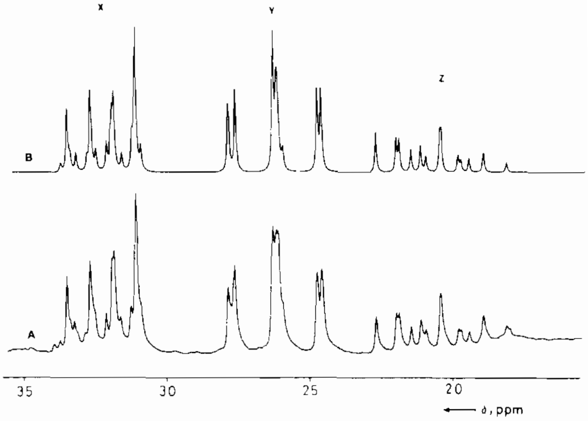

Fig. 1. ^1H NMR spectrum of $\{Mn[\overline{CH{-}CH_2{-}C(CN)_2{-}C(CN)_2{-}CH_2}](CO)_5\}$. (a) Experimental, in CD_2Cl_2 at 26 °C; (b) simulated spectrum.

TABLE I. ^1H NMR data for Cycloaddition Complex 2c in CD_2Cl_2 Solution at 26 °C; δ = ±0.04 ppm and J = ±0.2 Hz

$H_{A,A'}$	$H_{B,B'}$	H_C
3.21	2.58	1.99
$J_{A-B} = J_{A'-B'} = \mp 13.6$ $J_{A-A'} = \mp 1.7$ $J_{A-C} = J_{A'-C'} = \pm 6.9$ $J_{A-B'} = J_{A'-B} = \mp 0.4$	$J_{B-B'} = \mp 0.6$ $J_{B-C} = J_{B'-C} = \pm 13.3$	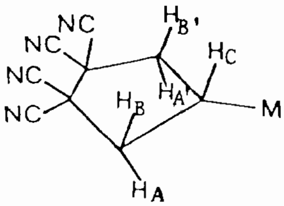

shows the numbering scheme for the protons (inset). These results confirm the occurrence of the cyclopentyl ring and the large difference between the J(A–C) and J(B–C) coupling constants [4] suggests a strongly asymmetric structure for the $-\overline{CHCH_2C(CN)_2C(CN)_2C}H_2$ moiety.

Mass Spectrometric Behavior of η^1-allyl Compounds 1a, 1b and 1c

The mass spectrum of **1a** is shown in Fig. 2a, the spectrum of **1b** is reported in Table II and the spectrum of **1c** is shown in Fig. 3. Compounds **1a** and **1c** give rise to scarcely abundant molecular ions whereas **1b** displays a $M^{+\bullet}$ with a relative abundance of 19%. These facts reasonably reflect the higher thermodynamic stability of **1b** produced by the rigid bis-phosphino chelating ligand. Compound **1b** turns out to be quite stable even in condensed phase, and it may be completely recovered after several hours in boiling toluene, in which *trans*-[PtCl(η^1-C_3H_5)(PPh_3)$_2$] (**1a**), undergoes extensive decomposition. Linked scans and exact mass measurements gave the fragmentation patterns reported in Schemes 1–3.

The EI decomposition of **1a** is strictly related to the cleavage of Pt–phosphine and σPt–allyl bonds. The base peak at m/z 262 is due to PPh_3^+, the ionic species at m/z 533 $[M-PPh_3]^{+\bullet}$, being complementary (Scheme 1). The η^3-allyl formulation proposed for the ion at m/z 533 is conceivable considering possible stabilization of the η^3-allyl bond after the loss of one neutral ligand. This hypothesis was confirmed by the mass spectrometric behavior of the complex [PtCl(η^3-C_3H_5)(PPh_3)], which displays the same fragmentation patterns as the ion at m/z 533 obtained from **1a** after release of PPh_3.

TABLE II. Mass Spectra m/z (relative absorbance)

1b	**1b**: 183(100.0), 184(21.0), 185(27.0), 186(8.0), 189(5.0), 205(60.0), 206(10.0), 207(9.0), 210(8.0), 212(11.0), 220(16.0), 221(5.0), 225(4.0), 226(10.0), 227(3.0), 240(4.0), 252(4.0), 262(14.0), 263(3.0), 281(5.0), 287(9.0), 288(4.0), 301(25.0), 302(28.0), 303(23.0), 304(4.0), 305(7.0), 332(3.0), 333(10.0), 334(8.0), 335(4.0), 345(2.0), 346(6.0), 347(8.0), 348(6.0), 349(3.0), 350(1.50), 375(4.0), 376(7.0), 377(7.0), 378(6.0), 379(1.5), 396(8.0), 397(2.0), 407(8.0), 408(10.0), 409(13.0), 410(11.0), 411(9.0), 412(2.0), 413(3.0), 432(2.0), 433(2.0), 434(4.0), 435(5.0), 436(2.0), 437(1.5), 453(2.5), 454(2.0), 455(3.0), 456(1.0), 483(2.0), 484(7.0), 485(6.0), 486(7.0), 487(2.0), 488(2.0), 588(2.0), 589(12.0), 590(13.0), 591(11.0), 592(4.0), 593(3.0), 594(1.0), 625(30.0), 626(30.0), 627(38.0), 628(19.0), 629(19.0), 630(4.0), 631(10.0), 632(10.0), 633(12.0), 634(2.5), 665(2.0), 666(19.0), 667(21.0), 668(32.0), 669(23.0), 670(23.0), 671(6.0), 672(4.0), 673(1.0). [PtCl(η^3-C_3H_5)(PPh_3)]: 261(26.0), 262(100.0), 263(46.0), 264(5.0), 265(1.0), 301(7.0), 302(8.0), 303(6.0), 304(1.0), 305(2.0), 311(1.0), 312(0.5), 313(3.0), 314(1.0), 375(5.0), 376(7.0), 377(15.0), 378(13.0), 379(15.0), 380(2.0), 453(2.0), 454(34.0), 455(36.0), 456(31.0), 457(2.0), 458(2.0), 531(4.0), 532(5.0), 533(6.0), 535(2.0).
2a	**2a**: 105(8.3), 106(13.3), 107(16.7), 108(33.3), 109(3.3), 115(11.7), 116(20.0), 117(8.3), 150(1.7), 151(0.8), 152(16.7), 153(8.3), 154(8.3), 183(83.0), 184(16.7), 185(8.3), 261(66.7), 262(100.0), 263(66.7), 280(8.3), 281(16.7), 282(8.3), 300(0.2), 301(0.8), 302(0.2), 321(2.5), 322(3.3), 323(2.5), 336(2.5), 337(6.7), 338(5.0), 358(1.0), 359(2.8), 360(1.3), 376(1.0), 377(1.8), 378(1.2), 401(1.0), 402(4.5), 403(2.5), 408(0.7), 409(2.0), 410(0.7), 428(0.5), 429(1.0), 430(0.5), 455(0.5), 456(0.7), 457(0.5), 478(0.2), 479(2.0), 480(0.1), 493(0.7), 494(2.2), 495(1.7), 593(0.5), 594(0.8), 595(0.7), 717(1.3), 718(8.3), 719(0.8), 720(1.7), 743(1.0), 744(1.7), 745(0.7), 752(0.7), 753(0.8), 754(0.5), 922(0.2), 923(0.1).
2b	**2b**: 183(100.0), 184(20.0), 185(15.0), 186(10.0), 201(20.0), 202(8.0), 203(5.0), 204(6.0), 205(6.0), 206(6.0), 207(13.0), 208(6.0), 209(5.0), 210(10.0), 211(5.0), 212(5.0), 217(5.0), 218(7.0), 219(25.0), 220(8.0), 221(6.0), 227(10.0), 228(5.0), 229(3.0), 230(8.0), 231(10.0), 232(9.0), 233(7.0), 244(10.0), 245(10.0), 246(20.0), 247(5.0), 247(5.0), 258(5.0), 259(5.0), 260(7.0), 261(5.0), 262(8.0), 263(4.0), 270(5.0), 271(8.0), 272(6.0), 273(3.0), 283(6.0), 284(2.0), 285(6.0), 286(5.0), 287(8.0), 288(2.0), 301(42.0), 302(45.0), 303(25.0), 304(5.0), 305(10.0), 313(7.0), 332(5.0), 333(10.0), 334(8.0), 335(11.0), 336(3.0), 337(2.0), 346(7.0), 347(8.0), 348(7.0), 349(3.0), 350(2.0), 351(25.0), 352(6.0), 353(2.0), 375(3.0), 376(4.0), 377(10.0), 378(9.0), 379(8.0), 380(2.0), 396(5.0), 397(2.0), 407(6.0), 408(6.0), 409(8.0), 410(12.0), 411(10.0), 412(9.0), 433(2.0), 434(4.0), 435(5.0), 436(5.0), 437(3.0), 438(2.0), 453(1.5), 454(2.5), 455(3.0), 456(4.0), 457(1.5), 483(1.5), 484(2.5), 485(5.5), 486(6.0), 487(5.0), 488(2.5), 489(1.5), 490(1.0), 511(2.0), 512(2.0), 513(3.5), 514(3.0), 515(2.0), 538(1.0), 539(1.5), 540(1.5), 541(0.5), 562(1.0), 563(1.5), 564(2.0), 565(2.3), 566(2.0), 567(1.5), 590(50.0), 591(54.0), 592(45.0), 593(10.0), 594(10.0), 595(4.0), 615(7.0), 616(20.0), 617(18.0), 618(14.0), 619(5.0), 620(5.0), 625(15.0), 626(15.0), 627(13.0), 628(8.0), 629(7.0), 651(3.0), 652(5.0), 653(4.0), 654(2.3), 655(2.0), 718(0.5), 719(0.7), 720(0.7), 721(0.2), 743(0.5), 744(0.7), 745(0.5), 794(0.01), 795(0.01).
2c	**2c**: 39(4.0), 40(2.0), 41(4.0), 50(1.0), 51(2.0), 52(2.0), 53(1.0), 55(100.0), 80(1.0), 81(10.0), 82(1.0), 83(6.0), 84(1.0), 111(6.0), 112(1.0), 116(15.0), 117(3.0), 118(1.0), 139(8.0), 143(4.0), 144(1.0), 146(11.0), 147(1.0), 167(11.0), 168(1.0), 169(14.0), 170(3.0), 171(2.0), 183(1.0), 195(9.0), 196(2.0), 197(5.0), 198(2.0), 211(2.0), 224(55.0), 225(7.0), 226(1.0), 239(2.0), 252(3.0), 267(0.5), 280(3.0), 295(1.5), 308(1.0), 323(12.0), 324(2.0), 336(1.0), 364(0.5).

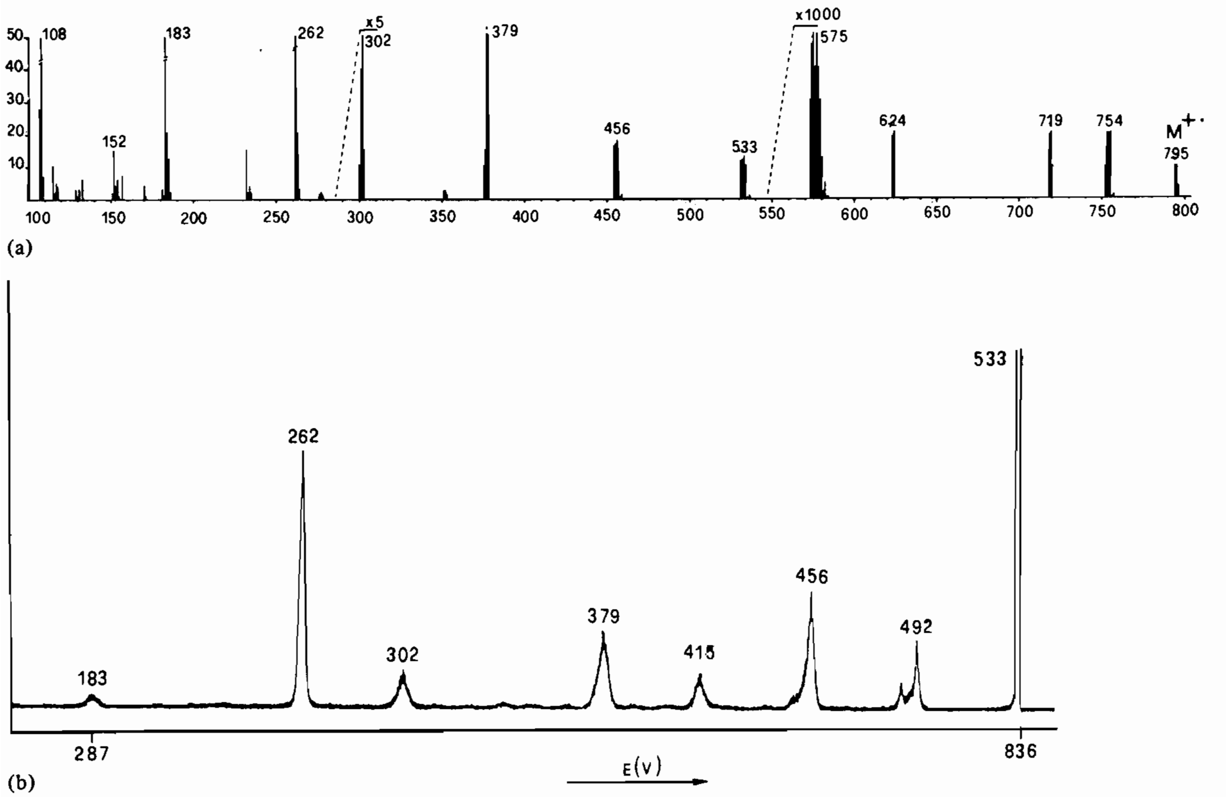

Fig. 2. (a) EI mass spectrum of **1a**. (b) CAD MIKE spectrum of ionic species at *m/z* 533 originated by EI of **1a**, identical to that of $M^{+\bullet}$ of $[PtCl(\eta^3\text{-}C_3H_5)(PPh_3)]$.

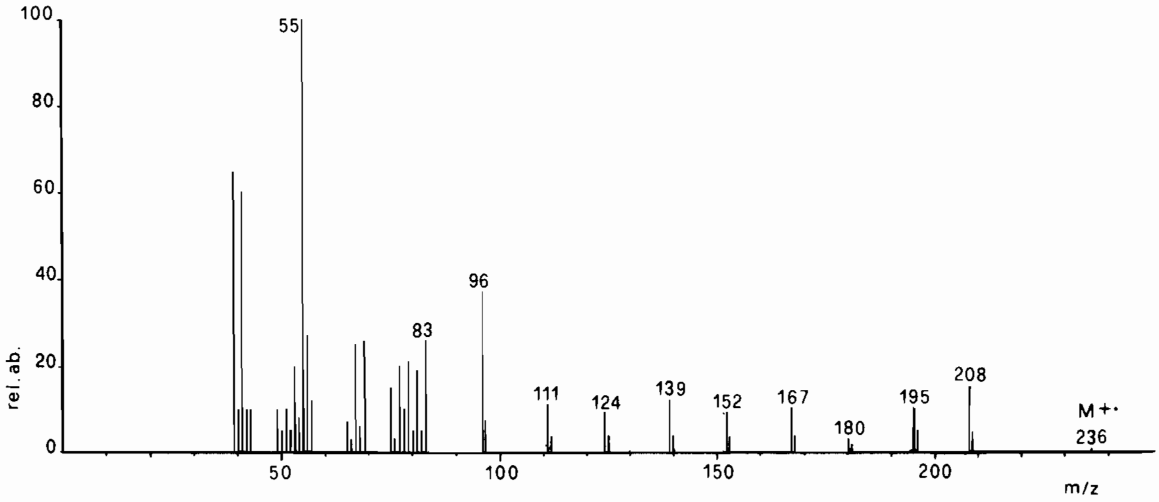

Fig. 3. EI mass spectrum of **1c**.

The CAD MIKE spectrum of ionic species at *m/z* 533 originating from EI of **1a** (Fig. 2b) is identical to that of the $M^{+\bullet}$ from $[PtCl(\eta^3\text{-}C_3H_5)(PPh_3)]$, thus proving the validity of our structure assignment. Sequential losses of two phenyl radicals from ions at *m/z* 533 lead to ionic species at *m/z* 379. A further contemporary metastable supported loss of HCl and $C_3H_5^{\bullet}$ leads to the ions at *m/z* 302 corresponding to $[C_6H_4PPt]^+$, for which we cannot offer a reasonable structural formulation. It is noteworthy that allyl group and HCl losses occur from the ion at *m/z* 379 and not from other ions at *m/z* 533 or 456, confirming the generality of the η^3-allyl stabilizing effect discussed above.

The alternative fragmentation pathway involving primary $C_3H_5^{\bullet}$ elimination and subsequent $Cl^{\bullet}$ loss

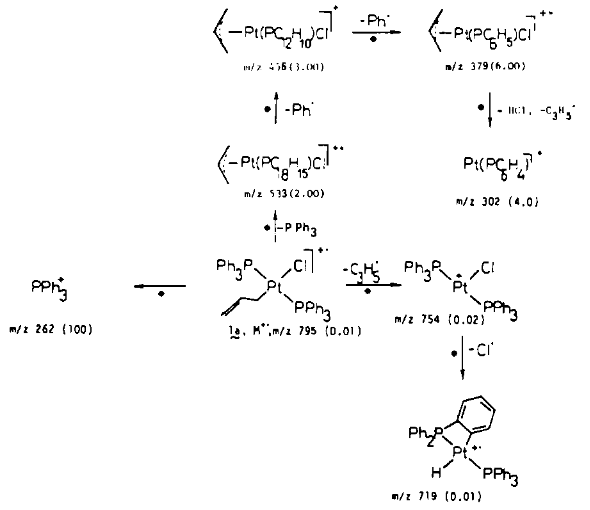

Scheme 1.

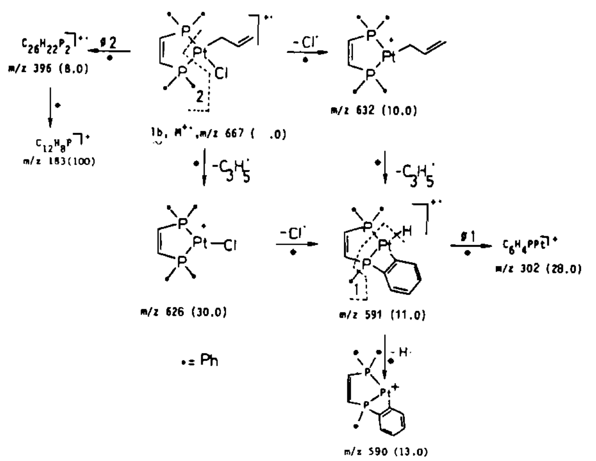

Scheme 2.

leading to a species at *m*/*z* 719, certainly displays relative abundances of fragment ions which are lower than those found for the path with primary PPh_3 loss. This fact agrees with the proposed η^3-allyl bond occurrence which may result in general stabilization of η^3-allyl fragment ions. Formulation for the ion at *m*/*z* 719 was based on transmetallation involving the phosphine phenyl rings [15–17].

Compound **1b** shows a substantially different mass spectrometric behavior; much more abundant high mass ions can reasonably be attributed to the stabilizing effect of the chelating bis-phosphino ligand, which remains firmly coordinated in most fragmentation species (Scheme 2). Primary $Cl^•$ and $C_3H_5^•$ losses lead to ions at *m*/*z* 632 and 626 respectively, allyl radical elimination being preferred as shown by the relative abundances (30:10) of ions at *m*/*z* 626 and 632 (the same ratio is also maintained in the B/E spectrum of $M^{+•}$).

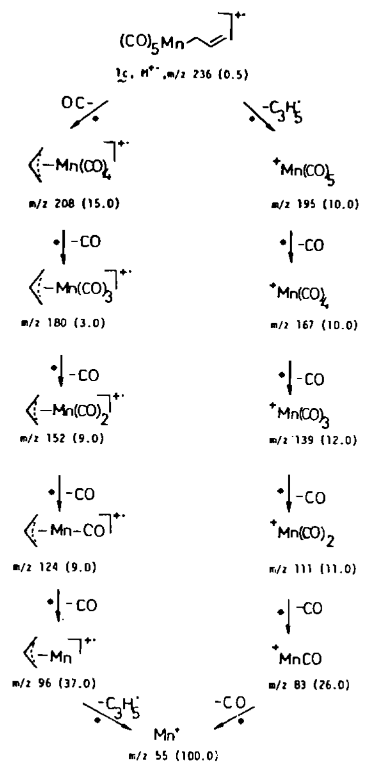

Scheme 3.

The results reflect the lower stability expected for the Pt–C σ bond compared with the Pt–Cl bond. The ions at *m*/*z* 626 decompose further, leading to ionic species at *m*/*z* 591 by $Cl^•$ loss and a possible *trans*-metallation reaction with the occurrence of a Pt–H bond. The hydride formation and the ortho-metallation reaction led us to study further the $|C_{26}H_{22}P_2Pt|^{+•}$ (*m*/*z* 591) ions. Their B/E linked scans and MIKE spectra show abundant $H^•$ loss, easily explained by the presence of hydride. Furthermore, the C_6H_4 loss is accompanied by a high energy release (202 meV) which may indicate the bond cleavage of a strained cyclic structure [14, 18]. The results thus confirm the structure assignments reported in Scheme 2. Interestingly, the final Pt containing fragmentation product is the ion at *m*/*z* 302, corresponding to $|C_6H_4PPt|^+$, which is the last Pt-containing ion also observed in the mass spectrum of **1a**. Structural collapse to this ion must involve a complex fragmentation process, with extensive skeletal rearrangement. For our purposes it was of interest that the chelating bis-phosphine prevented the appearance of the η^3-allyl bonding mode and, consequently loss of the allyl radical turns out to be the most important fragmentation path for the molecular ion.

In this connection, the case of $[Mn(\eta^1\text{-}C_3H_5)(CO)_5]$ (**1c**) may be significant: its mass spectrum is dominated by both CO and/or $C_3H_5^•$ releases as shown in Scheme 3 and Fig. 3. The molecular species alternatively loses the $C_3H_5^{\bullet}$ moiety or one CO, affording the ions at *m/z* 195 and 208 respectively, with very close relative abundances. By subsequent CO losses these species lead to $|MnCO|^+$ and $|MnC_3H_5|^{+\bullet}$ ions maintaining two independent paths. Consistently, Mn–CO bond breaking, a fragmentation path for metal carbonyls [19, 20], may result in η^3-allyl bond formation within the metal coordination sphere until the loss of CO ligands is complete. On the other, this does not exclude Mn–C σ bond breaking on the starting η^1-allyl complex. These results are in line with the already discussed cases of **1a** and **1b** and agree with the preparation of $[Mn(\eta^3\text{-}C_3H_5)(CO)_4]$ which occurs by loss of CO under reduced pressure [11].

Mass Spectrometric Behavior of Cycloaddition Products 2a, 2b and 2c

The EI mass spectra of cycloaddition products **2a**, **2b** and **2c** allow comparison with precursor species **1a**, **1b** and **1c** as to chemical stability and in terms of some preliminary considerations on the |2 + 3| cycloaddition mechanism (reaction (1)).

The mass spectra of species **2a** and **2b** (Table II) account for fragmentation Schemes 4 and 5 respectively. The overall pattern is substantially similar in both cases; the $\cdot\overline{\dot{C}H{-}CH_2{-}C(CN)_2{-}C(CN)_2{-}\dot{C}H_2}$ release governs the fragmentation path leading to ionic species at *m/z* 754 and 626 from $M^{+\bullet}$ of **2a** and $M^{+\bullet}$ of **2b** respectively. This fact indicates that for 2 Pt–C σ bond breaking is unaffected by the coordination environment of Pt. Once the η^1-allyl group is engaged with TCNE in 5-member ring formation, the special reactivity of the η^1-allyl ligand (whose suitability for η^3-allyl bonding depends on ancillary ligands [21]) disappears, in agreement with the similar behavior of **2a** and **2b**. These results on Pt(II) complexes deserve some comment in regard to the possible decomposition of the ring. Electron impact induced decomposition pathways of organic cycloaddition products often involve a retro-reaction [22, 23] which results in TCNE or allyl release from the precursor ion. This path cannot be invoked for Pt(II) complexes since the ionic species originated from the molecular ion of complexes type 2 by loss of TCNE or $C_3H_5^{\bullet}$, are absent. Consistently, retro-reactions, which are well-established mechanisms for classic organic cyclo-addition products, may be disfavoured in organometallic chemistry because of the weakness of the metal–carbon σ bond in comparison with the strength of the C–C bond [24]. On the other hand, the occurrence of fragments holding Pt–CN bonds (Schemes 4 and 5) may indicate release of the cyclic moiety as a neutral unsaturated molecule without skeletal rearrangements.

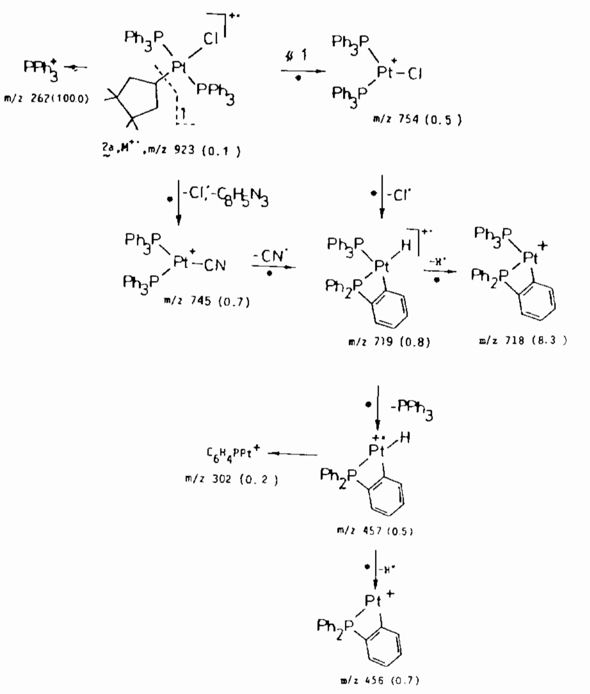

Scheme 4.

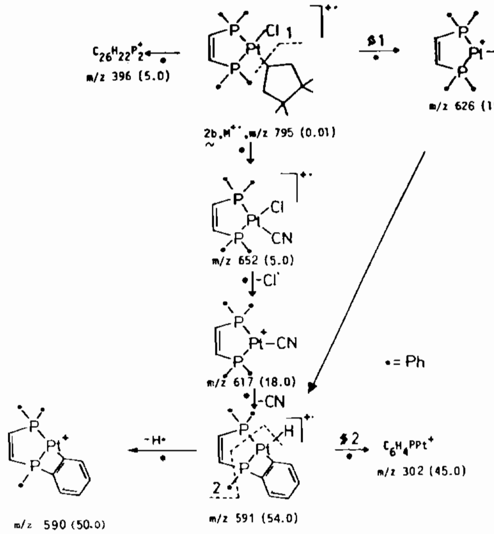

Scheme 5.

In contrast, an important skeletal rearrangement occurs in the case of $\{Mn[\overline{\dot{C}HCH_2C(CN)_2C(CN)_2\dot{C}H_2}](CO)_5\}$ (**2c**) (Scheme 6). While subsequent CO losses or $^{\bullet}\overline{\dot{C}HCH_2C(CN)_2C(CN)_2\dot{C}H_2}$ radical elimination from $M^{+\bullet}$ of **2c** may be explained on the same ground used for **2a**, **2b** and **1c** mass spectra, the presence of the ion at *m/z* 323, corresponding to $[Mn(TCNE)(CO)_5]^{+\bullet}$, unambiguously indicates the occurrence of the 5-membered ring decomposition with $C_3H_5^{\bullet}$ elimination and maintainance of TCNE. This different behavior in comparison with that

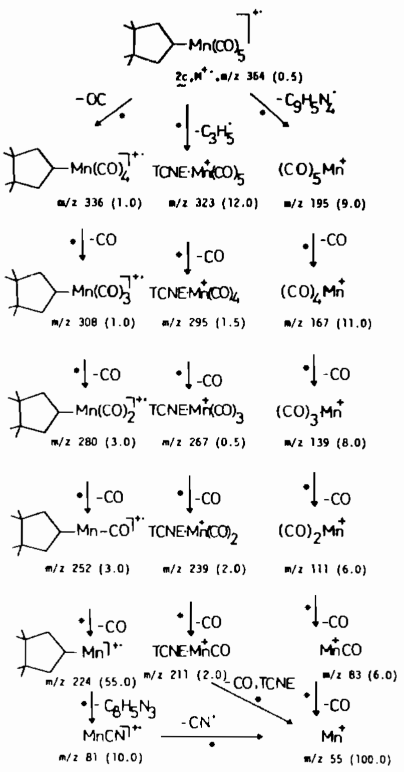

Scheme 6.

observed in the spectra of **2a** and **2b** is related to the energy release at the level of vibrational frequencies subsequent to electron impact: the uniformity of the coordination sphere composed of five CO surrounding the Mn(I) ion may direct the energy release onto the metal–C σ bond of $M^{+\bullet}$ of **2c** overwhelming the α carbon and giving rise to skeletal rearrangements of the 5-membered ring. This does not prevent either Mn–C σ bond breaking or subsequent CO losses.

References

1 A. Wojcicki, in M. Tsutsui, Y. Ishii and Y. Huang (eds.), 'Fundamental Research in Organometallic Chemistry', Van Nostrand-Reinhold, New York, 1982, pp. 569–597.

2 M. Calligaris, G. Nardin, G. Carturan and A. Wojcicki, *Inorg. Chim. Acta, 54,* L285 (1981).

3 M. Rosemblum, *Acc. Chem. Res., 7,* 122 (1974).

4 M. Calligaris, G. Carturan, G. Nardin, A. Scrivanti and A. Wojcicki, *Organometallics, 2,* 865 (1983).

5 A. P. Bruins, K. R. Jennings and S. Evans, *Int. J. Mass Spectrom. Ion Phys., 26,* 395 (1978).

6 C. J. Porter, J. H. Beynon and T. Ast, *Org. Mass Spectrom., 16,* 101 (1981).

7 D. F. Shriver, 'The Manipulation of Air-Sensitive Compounds', McGraw-Hill, New York, 1969.

8 D. D. Perrin, W. L. F. Armarego and D. R. Perrin, 'Purification of Laboratory Chemicals', Pergamon, Oxford, U.K., 1966.

9 J. H. Lukas, *Inorg. Synth., 15,* 75 (1974).

10 B. E. Mann, B. L. Shaw and G. Shaw, *J. Chem. Soc. A,* 3536 (1971).

11 W. R. McClellan, H. N. Hoen, H. N. Cripps, E. L. Muetterties and B. W. Howk, *J. Am. Chem. Soc., 83,* 1601 (1961).

12 R. P. Morgan, G. H. Beynon, R. H. Bateman and B. N. Green, *J. Mass Spectrom. Ion Phys., 28,* 171 (1979).

13 P. Traldi, U. Vettori and F. Dragoni, *Org. Mass Spectrom., 17,* 587 (1982).

14 R. G. Cooks, J. H. Beynon, R. M. Caprioli and G. R. Lester, in 'Metastable Ions', Elsevier, Amsterdam, 1973, Appendix IV.

15 P. Traldi, U. Vettori, A. L. Banditelli and L. Minghetti, *Inorg. Chim. Acta, 69,* 207 (1983).

16 P. Traldi, U. Vettori, G. Banditelli, A. L. Bandini and L. Minghetti, to be published.

17 F. Glokling, T. McBride and R. J. I. Pollock, *Inorg. Chim. Acta, 8,* 81 (1974).

18 F. R. Hartley, 'The Chemistry of Platinum and Palladium', Applied Science, London, 1973, p. 156.

19 M. R. Litzow and T. R. Spalding, in M. F. Lappert (ed.), 'Mass Spectrometry of Inorganic and Organometallic Compounds', Elsevier, Amsterdam, 1973; J. Charambolous (ed.), 'Mass Spectrometry of Metal Compounds', Butterworths, London, 1975.

20 J. Muller and M. Herberhold, *J. Organomet. Chem., 13,* 399 (1968); J. Muller and K. Fenderl, *J. Organomet. Chem., 19,* 123 (1969).

21 S. Numata, R. Okawara and H. Kurosawa, *Inorg. Chem., 16,* 1737 (1977); N. M. Boag, M. Green, J. L. Spencer and F. G. A. Stone, *J. Chem. Soc., Dalton Trans.,* 1208 (1980); G. Carturan, A. Scrivanti, U. Belluco and F. Morandini, *Inorg. Chim. Acta, 26,* 1 (1978); *27,* 37.

22 A. Selva, P. Traldi and P. Fantucci, in N. R. Daly (ed.), 'Advanced Mass Spectrometry', Vol. 7, Heyden, London, 1978, p. 1204.

23 T. Kametani and F. Fukumoto, *Acc. Chem. Res., 9,* 319 (1976).

24 J. Halpern, *Acc. Chem. Res., 15,* 238 (1982).